Hamiltonian effective field theory with the nucleon excitations and kaonic deuteron

Zhan-Wei Liu

School of Physical Science and Technology, Lanzhou University

Collaborators: Dan Guo, Johnathan M. M. Hall, Waseem Kamleh, Derek B. Leinweber, Finn M. Stokes, Anthony W. Thomas, Jia-Jun Wu

CONTENTS

The Nucleon Excitations with Hamiltonian EFT

Hadron Physics

mainly focused on hadron scatterings, spectra, structures, interactions, etc.

mainly focused on hadron scatterings, spectra, structures, interactions, etc.

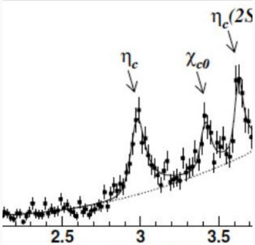

Hadron Physics

mainly focused on hadron scatterings, spectra, structures, interactions, etc.

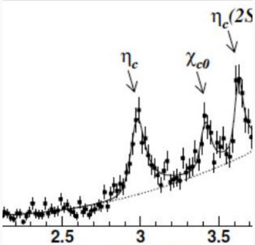

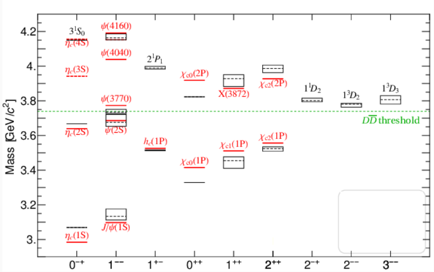

Hadron Physics

mainly focused on hadron scatterings, spectra, structures, interactions, etc.

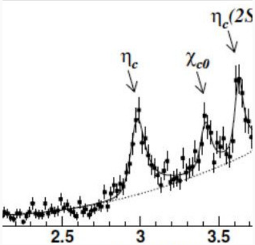

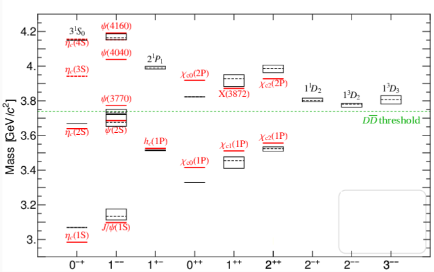

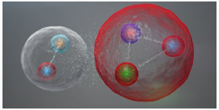

Hadron Physics

mainly focused on hadron scatterings, spectra, structures, interactions, etc.

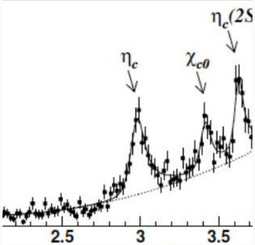

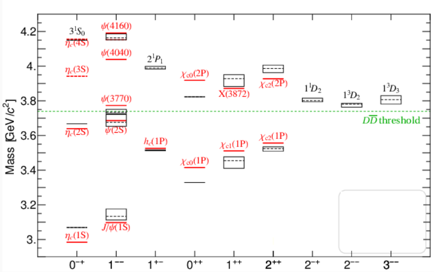

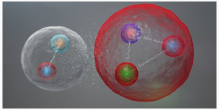

traditional perturbation expansion in series of $(\alpha_s)^n$?

Hadron Physics

mainly focused on hadron scatterings, spectra, structures, interactions, etc.

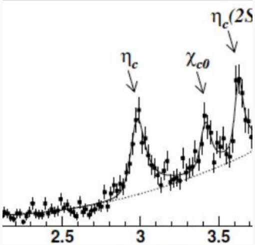

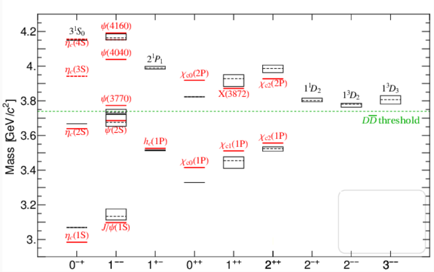

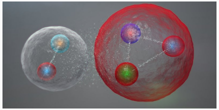

traditional perturbation expansion in series of $(\alpha_s)^n$?

- constituent quark model
- effective field theory
- lattice QCD
- QCD sum rule
- large Nc
- ...

Hadron Physics

mainly focused on hadron scatterings, spectra, structures, interactions, etc.

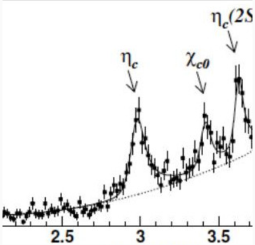

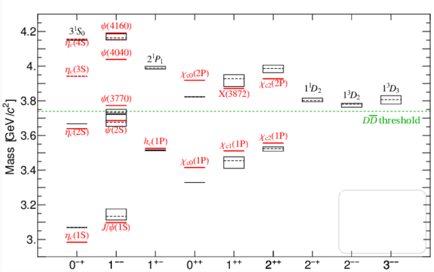

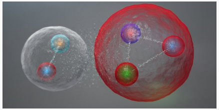

traditional perturbation expansion in series of $(\alpha_s)^n$?

- constituent quark model
- effective field theory
- lattice QCD
- QCD sum rule
- large Nc
- ...

Lattice QCD

- LQCD starts from the first principle of QCD
- model independent, reliable
- LQCD gives hadron spectra and quark distribution functions

  at finite volumes, large quark masses, discrete spaces
- not directly related to physical observables

Connection between Scattering Data and Lattice QCD Data

Lattice QCD

- large pion mass: extrapolation
- finite volume
- discrete space

Lattice QCD Data → Physical Data

- Lüscher Formalisms and extensions:

  Model independent; efficient in single-channel problems

    Spectrum → Phaseshifts;
- Effective Field Theory (EFT), Models, etc

  with low-energy constants fitted by Lattice QCD data

Physical Data → Lattice QCD Data

- EFT: discretization, analytic extension, Lagrangian modification
- various discretization: eg. discretize the momentum in the loop

Lattice QCD and Effective Field Theory

Effective field theory deals with extrapolation powerfully.

Finite-volume effect can be studied by discretizing the EFT.

Discrete spacing effects can also be studied with EFT.

Scattering Data and Lattice QCD data are two important sources for studying resonances.

We should try to analyse them both at the same time.

Hamiltonian Effective Field Theory

Hamiltonian Effective Field Theory (HEFT)

analyses both experimental data at infinite volume

and lattice QCD results at finite volume at the same time.

Hamiltonian Effective Field Theory

Hamiltonian Effective Field Theory (HEFT)

analyses both experimental data at infinite volume

and lattice QCD results at finite volume at the same time.

- at infinite volume

Hamiltonian Effective Field Theory

Hamiltonian Effective Field Theory (HEFT)

analyses both experimental data at infinite volume

and lattice QCD results at finite volume at the same time.

- at infinite volume

  Lagrangian (via 2-particle irreducible diagrams) $\rightarrow$

Hamiltonian Effective Field Theory

Hamiltonian Effective Field Theory (HEFT)

analyses both experimental data at infinite volume

and lattice QCD results at finite volume at the same time.

- at infinite volume

  Lagrangian (via 2-particle irreducible diagrams) $\rightarrow$

  potentials (via Betha-Salpeter Equation) $\rightarrow$

Hamiltonian Effective Field Theory

Hamiltonian Effective Field Theory (HEFT)

analyses both experimental data at infinite volume

and lattice QCD results at finite volume at the same time.

- at infinite volume

  Lagrangian (via 2-particle irreducible diagrams) $\rightarrow$

  potentials (via Betha-Salpeter Equation) $\rightarrow$

  phaseshifts and inelasticities

Hamiltonian Effective Field Theory

Hamiltonian Effective Field Theory (HEFT)

analyses both experimental data at infinite volume

and lattice QCD results at finite volume at the same time.

- at infinite volume

  Lagrangian (via 2-particle irreducible diagrams) $\rightarrow$

  potentials (via Betha-Salpeter Equation) $\rightarrow$

  phaseshifts and inelasticities

- at finite volume

Hamiltonian Effective Field Theory

Hamiltonian Effective Field Theory (HEFT)

analyses both experimental data at infinite volume

and lattice QCD results at finite volume at the same time.

- at infinite volume

  Lagrangian (via 2-particle irreducible diagrams) $\rightarrow$

  potentials (via Betha-Salpeter Equation) $\rightarrow$

  phaseshifts and inelasticities

- at finite volume

  potentials discretized (via Hamiltonian Equation)$\rightarrow$ spectra

Hamiltonian Effective Field Theory

Hamiltonian Effective Field Theory (HEFT)

analyses both experimental data at infinite volume

and lattice QCD results at finite volume at the same time.

- at infinite volume

  Lagrangian (via 2-particle irreducible diagrams) $\rightarrow$

  potentials (via Betha-Salpeter Equation) $\rightarrow$

  phaseshifts and inelasticities

- at finite volume

  potentials discretized (via Hamiltonian Equation)$\rightarrow$ spectra

  wavefunctions: analyse the structure of the eigenstates on the lattice

Hamiltonian Effective Field Theory

Hamiltonian Effective Field Theory (HEFT)

analyses both experimental data at infinite volume

and lattice QCD results at finite volume at the same time.

- at infinite volume

  Lagrangian (via 2-particle irreducible diagrams) $\to$

  potentials (via Betha-Salpeter Equation) $\to$

  phaseshifts and inelasticities

- at finite volume

  potentials discretized (via Hamiltonian Equation)$\to$ spectra

  wavefunctions: analyse the structure of the eigenstates on the lattice

- finite-volume and infinite-volume results are connected by the coupling constants etc.

$N^*(1535)$ with πN Scattering

$N^*(1535)$ is the lowest resonance with $I(J^P) = \frac{1}{2}(\frac{1}{2}^-)$.

- One needs to consider the interactions

  among the bare baryon N_0^*, πN channel, and ηN channel.

$$G^2_{\pi N;N_0^*}(k) = \frac{3g^2_{\pi N;N_0^*}}{4\pi^2 f^2}\omega_\pi(k)$$

$$V^S_{\pi N,\pi N}(k,k') = \frac{3g^S_{\pi N}}{4\pi^2 f^2}\frac{m_\pi + \omega_\pi(k)}{\omega_\pi(k)}\frac{m_\pi + \omega_\pi(k')}{\omega_\pi(k')}$$

- Phase shifts and inelasticities

  are obtained by solving Bethe-Salpeter equation with the interactions.

$$T_{\alpha,\beta}(k,k';E) = V_{\alpha,\beta}(k,k') + \sum_\gamma \int q^2 dq$$

$$V_{\alpha,\gamma}(k,q)\frac{1}{E - \sqrt{m^2_{\gamma_1} + q^2} - \sqrt{m^2_{\gamma_2} + q^2} + i\epsilon}T_{\gamma,\beta}(q,k';E)$$

$N^*(1535)$ with πN scattering at infinite volume

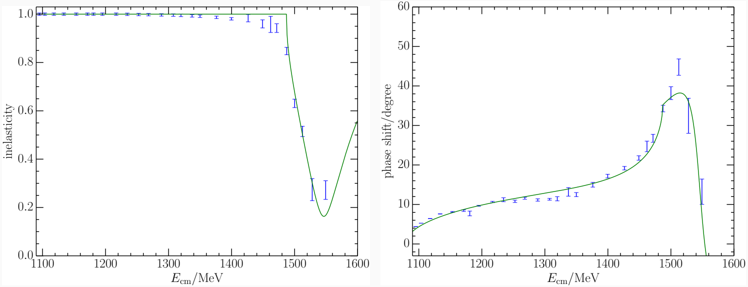

πN Scattering with $I(J^P) = \frac{1}{2}(\frac{1}{2}^-)$.

Our Pole: $1531 \pm 29 -$ i 88 ± 2 MeV.

Particle Data Group: $1510 \pm 20 -$ i 85 ± 40 MeV.

Discretization in finite volume

$$H_0 = \mathrm{diag}\{m^0_{N_1}, \omega_{\pi N}(k_0),\ \omega_{\eta N}(k_0), \omega_{\pi N}(k_1),\ \omega_{\eta N}(k_1), ...\},$$

$$H_I = \begin{pmatrix} 0 & \tilde{G}_{\pi N}(k_0) & \tilde{G}_{\eta N}(k_0) & \tilde{G}_{\pi N}(k_1) & \tilde{G}_{\eta N}(k_1) & \dots \\ \tilde{G}_{\pi N}(k_0) & \tilde{V}^S_{\pi N,\pi N}(k_0, k_0) & 0 & \tilde{V}^S_{\pi N,\pi N}(k_0, k_1) & 0 & \dots \\ \tilde{G}_{\eta N}(k_0) & 0 & 0 & 0 & 0 & \dots \\ \tilde{G}_{\pi N}(k_1) & \tilde{V}^S_{\pi N,\pi N}(k_1, k_0) & 0 & \tilde{V}^S_{\pi N,\pi N}(k_1, k_1) & 0 & \dots \\ \tilde{G}_{\eta N}(k_1) & 0 & 0 & 0 & 0 & \dots \\ \vdots & \vdots & \vdots & \vdots & \vdots & \ddots \end{pmatrix},$$

where

$$\tilde{G}_i(k_n) = \sqrt{\frac{C_3(n)}{4\pi}} (\frac{2\pi}{L})^{3/2} G_i(k_n),$$

$$\tilde{V}^S_{i,j}(k_n, k_m) = \frac{\sqrt{C_3(n)C_3(m)}}{4\pi} (\frac{2\pi}{L})^3 V^S_{i,j}(k_n, k_m).$$

$C_3(n)$ represents the number of summing the squares of three integers to equal n.

Spectra at Finite Volumes

3 sets of lattice data at different pion masses and finite volumes

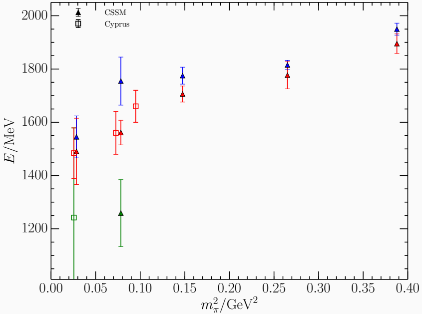

$L \approx 3$ fm

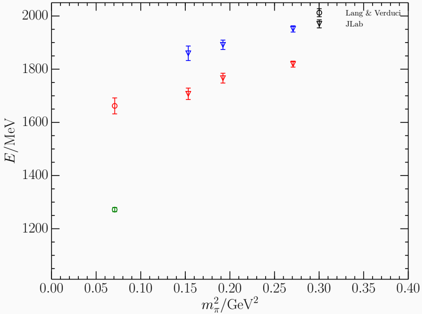

$L \approx 2$ fm

Spectra with $I(J^P) = \frac{1}{2}(\frac{1}{2}^-)$ at finite volumes

Spectra at Finite Volumes

3 sets of lattice QCD data at different pion masses and finite volumes

Non-interacting energies of the two-particle channels

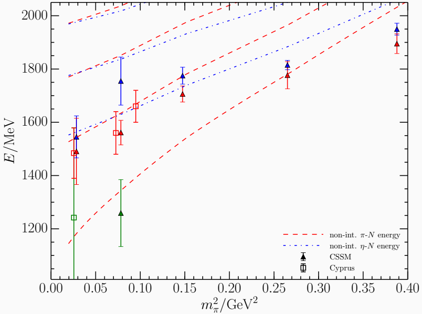

$L \approx 3$ fm

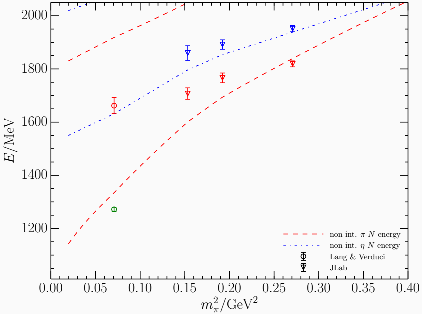

$L \approx 2$ fm

Spectra with $I(J^P) = \frac{1}{2}(\frac{1}{2}^-)$ at finite volumes

Spectra at Finite Volumes

3 sets of lattice QCD data at different pion masses and finite volumes

Non-interacting energies of the two-particle channels

Eigenenergies of Hamiltonian effective field theory

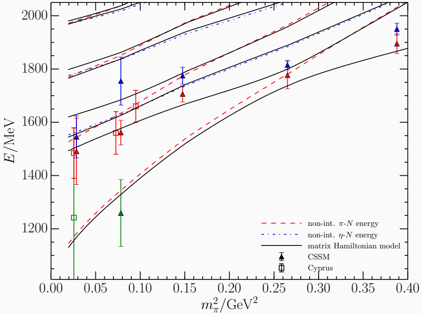

$L \approx 3$ fm

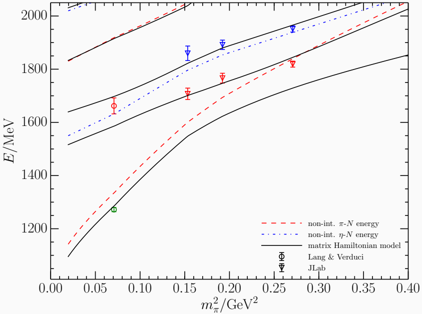

$L \approx 2$ fm

Spectra with $I(J^P) = \frac{1}{2}(\frac{1}{2}^-)$ at finite volumes

Spectra at Finite Volumes

3 sets of lattice data at different pion masses and finite volumes

Eigenenergies of Hamiltonian effective field theory

Coloured lines indicating most probable states observed in LQCD

We not only provide the mass but also analyze why some states are observed on the lattice

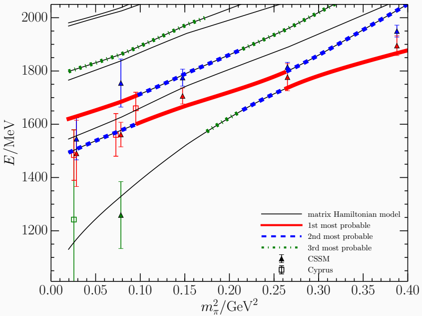

$L \approx 3$ fm

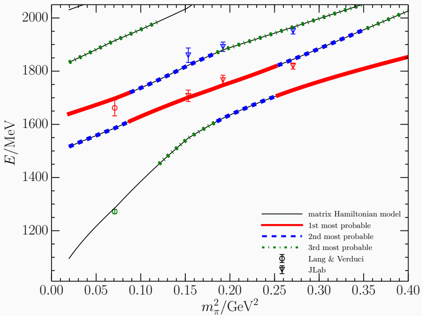

$L \approx 2$ fm

Spectra with $I(J^P) = \frac{1}{2}(\frac{1}{2}^-)$ at finite volumes

For more details, please see the following references:

Z. W. Liu, W. Kamleh, D. B. Leinweber, F. M. Stokes, A. W. Thomas and J. J. Wu, "Hamiltonian effective field theory study of the **N***(**1535**) resonance in lattice QCD," Phys. Rev. Lett. **116** (2016) no.8, 082004

Z. W. Liu, W. Kamleh, D. B. Leinweber, F. M. Stokes, A. W. Thomas and J. J. Wu, "Hamiltonian effective field theory study of the **N***(**1440**) resonance in lattice QCD," Phys. Rev. D **95** (2017) no.3, 034034

J. j. Wu, D. B. Leinweber, Z. w. Liu and A. W. Thomas, "Structure of the Roper Resonance from Lattice QCD Constraints," Phys. Rev. D **97** (2018) no.9, 094509

Components of Eigenstates with $L \approx 3$ fm

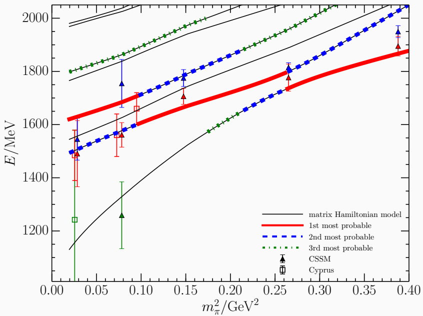

Spectra with $I(J^P) = \frac{1}{2}(\frac{1}{2}^-)$ and $L \approx 3$ fm

- The 1st eigenstate at light quark masses is mainly πN scattering states.
- The most probable state at physical quark mass is the 4th eigenstate.

  It contains about 60% bare $N^*(1535)$, 20% πN and 20% ηN.

Components of Eigenstates with $L \approx 3$ fm

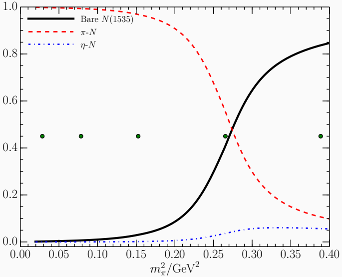

1st eigenstate

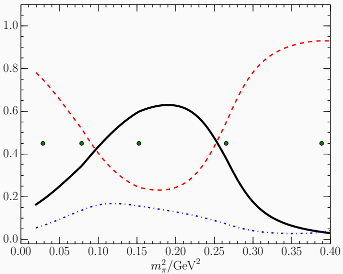

2nd eigenstate

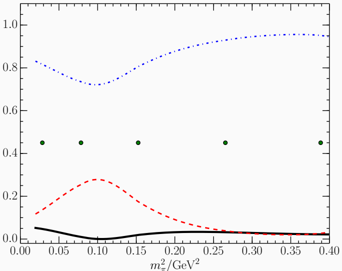

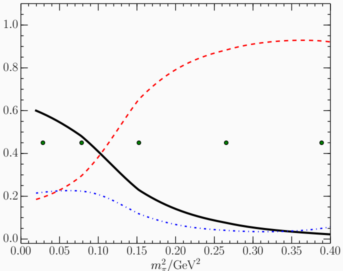

$N^*(1440)$ Resonance

- $N^*(1440)$, usually called Roper, is the excited state $I(J^P) = \frac{1}{2}(\frac{1}{2}^+)$
- Naive quark model predicts $m_{N^*(1440)} > m_{N^*(1535)}$
  if they are both dominated by 3-quark core. But contrary to experiment.

To check whether a 3-quark core largely exists in Roper, we consider models

- with a bare Roper
- without any bare baryons
- including the effect of the bare nucleon

$N^*(1440)$ Resonance

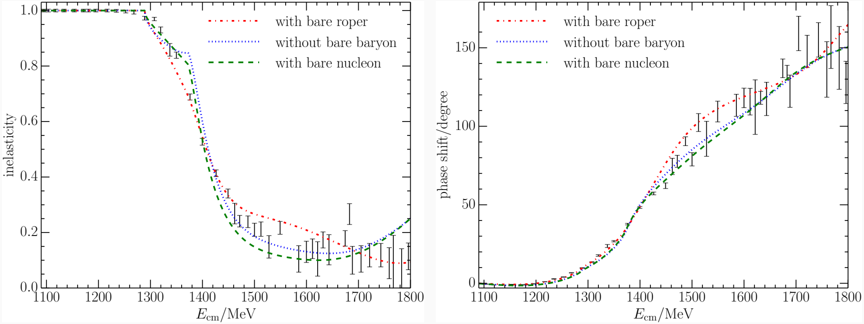

πN scattering with $I(J^P) = \frac{1}{2}(\frac{1}{2}^+)$

- with a bare Roper
- without any bare baryons
- including the effect of the bare nucleon

An original figure from later lattice QCD work

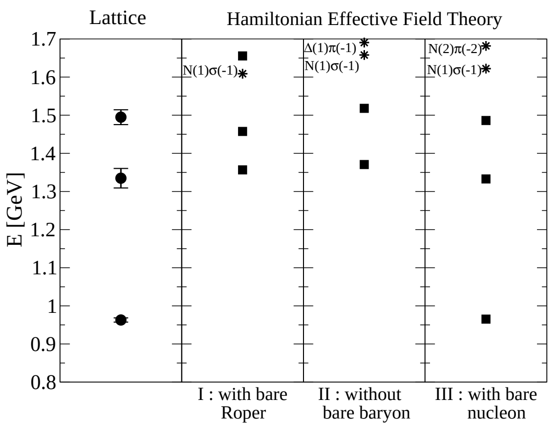

interpolating operators: $N(0)$, $N(0)\sigma(0)$, $N(p)\pi(-p)$, $\Delta(p)\pi(-p)$.

from Lang, Leskovec, Padmanath, Prelovsek, PRD95 (2017) no.1, 014510.

Pion Photoproduction off Nucleon with Hamiltonian EFT

Pion Photoproduction off Nucleon with Hamiltonian EFT

- combining
  - $\pi N \to \pi N$
  - lattice QCD data
  - $\gamma + N \to \pi + N$

Pion Photoproduction off Nucleon with Hamiltonian EFT

- combining
  - $\pi N \to \pi N$
  - lattice QCD data
  - $\gamma + N \to \pi + N$
- $\gamma + N \to \pi + N$

Pion Photoproduction off Nucleon with Hamiltonian EFT

- combining
  - $\pi N \to \pi N$
  - lattice QCD data
  - $\gamma + N \to \pi + N$
- $\gamma + N \to \pi + N$
  - γNN etc. couplings are not adjusted

Pion Photoproduction off Nucleon with Hamiltonian EFT

- combining
  - $\pi N \to \pi N$
  - lattice QCD data
  - $\gamma + N \to \pi + N$

- $\gamma + N \to \pi + N$
  - γNN etc. couplings are not adjusted
  - 

Pion Photoproduction off Nucleon with Hamiltonian EFT

- combining
  - $\pi N \to \pi N$
  - lattice QCD data
  - $\gamma + N \to \pi + N$

- $\gamma + N \to \pi + N$
  - γNN etc. couplings are not adjusted
  - 

$$\begin{aligned}\mathcal{M}(\gamma N \to \pi N) \quad \sim \quad & \mathcal{M}^{\mathrm{EM}}(\gamma N \to \pi N) \\ & + \mathcal{M}^{\mathrm{EM}}(\gamma N \to \pi N) \otimes \mathcal{M}^{\mathrm{FSI}}(\pi N \to \pi N) \\ & + \mathcal{M}^{\mathrm{EM}}(\gamma N \to \eta N) \otimes \mathcal{M}^{\mathrm{FSI}}(\eta N \to \pi N)\end{aligned}$$

Pion Photoproduction off Nucleon with Hamiltonian EFT

- combining
  - $\pi N \to \pi N$
  - lattice QCD data
  - $\gamma + N \to \pi + N$

- $\gamma + N \to \pi + N$
  - γNN etc. couplings are not adjusted
  - 

$$\mathcal{M}(\gamma N \to \pi N) \sim \mathcal{M}^{\mathrm{EM}}(\gamma N \to \pi N) + \mathcal{M}^{\mathrm{EM}}(\gamma N \to \pi N) \otimes \mathcal{M}^{\mathrm{FSI}}(\pi N \to \pi N) + \mathcal{M}^{\mathrm{EM}}(\gamma N \to \eta N) \otimes \mathcal{M}^{\mathrm{FSI}}(\eta N \to \pi N)$$

  - understand the structure of $N(1535)$ and the interactions of $\pi N/\eta N$ at low energies and near the resonance

Pion Photoproduction off Nucleon with Hamiltonian EFT

- combining
  - $\pi N \to \pi N$
  - lattice QCD data
  - $\gamma + N \to \pi + N$

- $\gamma + N \to \pi + N$
  - γNN etc. couplings are not adjusted
  - 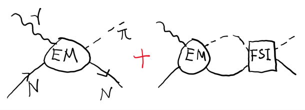

$$\begin{aligned}\mathcal{M}(\gamma N \to \pi N) \quad \sim \quad & \mathcal{M}^{\mathrm{EM}}(\gamma N \to \pi N) \\ & + \mathcal{M}^{\mathrm{EM}}(\gamma N \to \pi N) \otimes \mathcal{M}^{\mathrm{FSI}}(\pi N \to \pi N) \\ & + \mathcal{M}^{\mathrm{EM}}(\gamma N \to \eta N) \otimes \mathcal{M}^{\mathrm{FSI}}(\eta N \to \pi N)\end{aligned}$$

  - understand the structure of $N(1535)$ and the interactions of $\pi N/\eta N$ at low energies and near the resonance
  - necessities for the photon-nucleus investigation

Electromagnetic Multipoles

- $|\gamma N\rangle \rightarrow |\phi\,(\vec{k}),\; N(-\vec{k}, s_z'^N)\rangle,$ $k_x, k_y, k_z, s_z'^N$
- $|\gamma N\rangle \rightarrow |\phi\, N; k, J, J_z, L\rangle$, $k,\; J,\; J_z,\; L$
- $|\gamma N\rangle \rightarrow |\phi\, N; k, J, J_z, \lambda_N'\rangle$, $k,\; J,\; J_z, \lambda_N'$

Electromagnetic Multipoles

- $|\gamma N\rangle \to |\phi(\vec{k}),\ N(-\vec{k}, s_z'^N)\rangle$, $\quad$ $k_x, k_y, k_z, s_z'^N$
- $|\gamma N\rangle \to |\phi N; k, J, J_z, L\rangle$, $\quad$ $k,\ J,\ J_z,\ L$
- $|\gamma N\rangle \to |\phi N; k, J, J_z, \lambda_N'\rangle$, $\quad$ $k,\ J,\ J_z, \lambda_N'$

$$V_{\alpha,\gamma N}(J, \lambda_N', \lambda_\gamma, \lambda_N; k, q) = 2\pi \int_{-1}^{1} \mathrm{d}(\cos\theta) \sum_{s_z'^N} d^J_{\lambda_\gamma-\lambda_N,-\lambda_N'}(\theta) d^{1/2}_{s_z'^N,-\lambda_N'}(\theta)^* \mathcal{M}_{\alpha,\gamma N}(s_z'^N, \lambda_N, \lambda_\gamma; \vec{k}, \vec{q}),$$

$$V^{JLS;\lambda_\gamma\lambda_N}_{\alpha,\gamma N}(k,q) \quad = \quad \sqrt{\frac{2L+1}{2J+1}} \sum_{\lambda_N'} \langle L, S, 0, -\lambda_N' | J, -\lambda_N'\rangle \times V_{\alpha,\gamma N}(J, \lambda_N', \lambda_\gamma, \lambda_N; k, q).$$

D. Guo and Z. W. Liu, Phys. Rev. D **105** (2022) no.11, 11

Numerical results

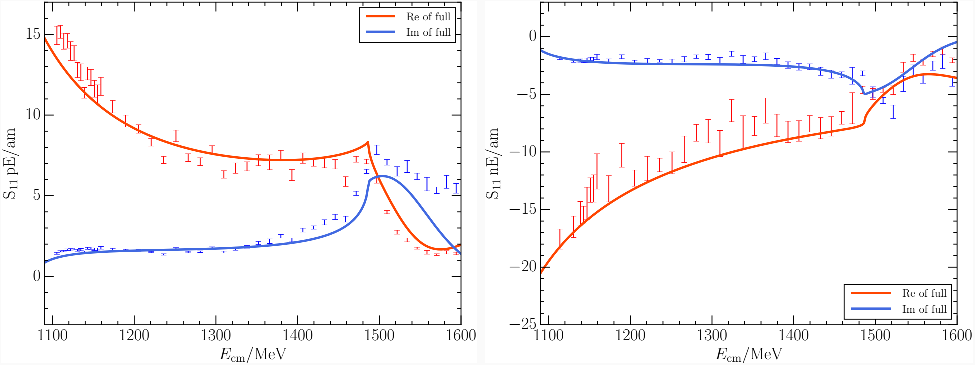

The bare core in $N^*(1535)$

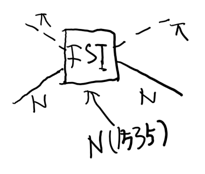

The bare core in $N^*(1535)$

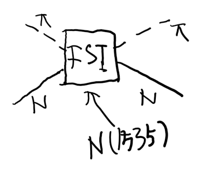

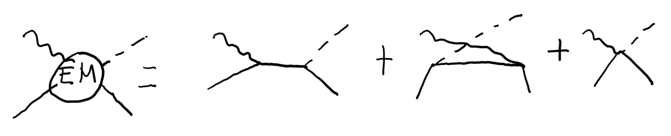

$+\dots$

The bare core in $N^*(1535)$

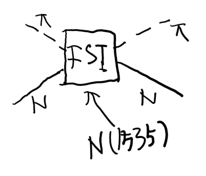

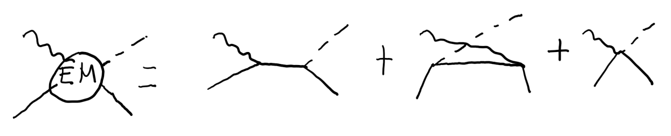

$+\dots$

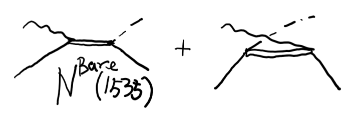

The bare core in $N^*(1535)$ cannot be absent in pion photoproduction

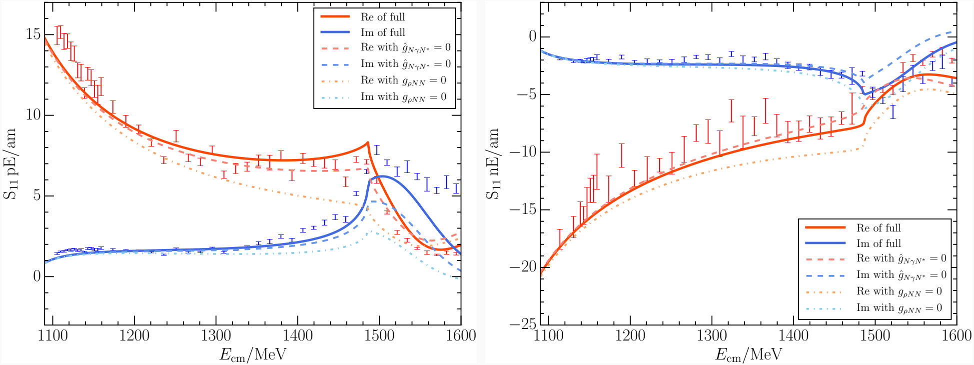

Estimation of the $N^*(1650)$ contribution

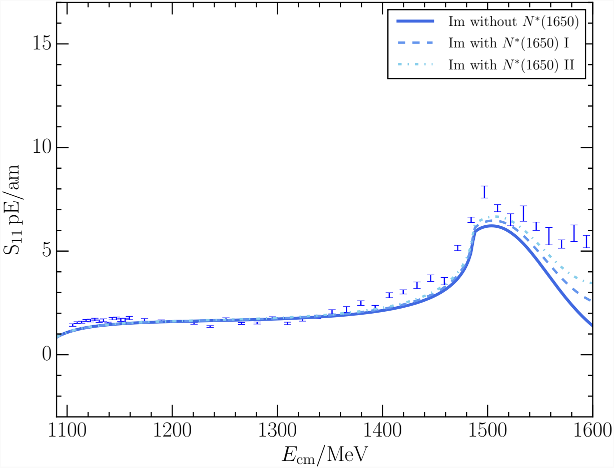

Estimation of the $N^{*}(1650)$ contribution

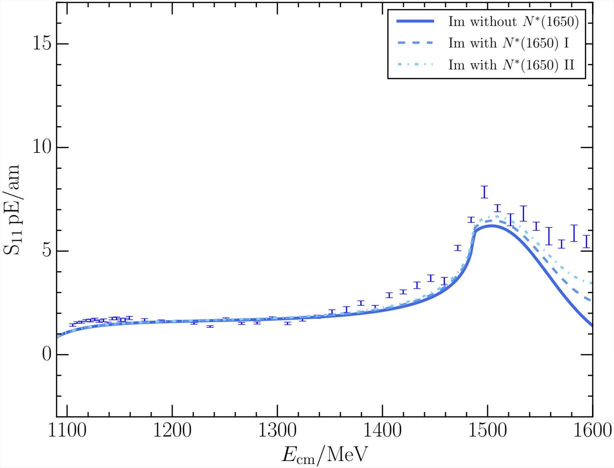

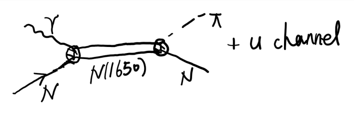

Kaonic Hydrogen and Deuteron with Hamiltonian EFT

$\Lambda(1405)$ with $K^- p$ scattering

- The well-known Weinberg-Tomozawa potentials are used.

  momentum-dependent, non-separable

$$v^I = \sum_{\alpha,\beta} \int d^3\vec{k}\, d^3\vec{k}'\, |\alpha(\vec{k})\rangle\, V^I_{\alpha,\beta}(k,k')\, \langle\beta(\vec{k}')|\,,$$

$$V_{\alpha,\beta}(k,k') = g_{\alpha,\beta} \frac{\omega_{\alpha_M}(k) + \omega_{\beta_M}(k')}{8\pi^2 f^2 \sqrt{2\omega_{\alpha_M}(k)}\sqrt{\omega_{\beta_M}(k')}}$$

$|\alpha\rangle = |\pi\Sigma\rangle,\ |\bar{K}N\rangle,\ |\eta\Lambda\rangle,\ |K\Xi\rangle,\ |\pi\Lambda\rangle$

- two scenarios: with or without a bare baryon

$$g^I = \sum_{\alpha,B_0} \int d^3\vec{k}\, \left\{ |\alpha(\vec{k})\rangle\, G^{I\dagger}_{\alpha,B_0}(k)\, \langle B_0| + |B_0\rangle\, G^I_{\alpha,B_0}(k)\, \langle\alpha(\vec{k})| \right\},$$

where

$$G^I_{\alpha,B_0}(k) = \frac{\sqrt{3}\, g^I_{\alpha,B_0}}{2\pi f} \sqrt{\omega_\pi(k)}\ u(k).$$

$$H^I_{\rm int} = g^I + v^I.$$

$\Lambda(1405)$ with $K^- p$ scattering

We can fit the cross sections of $K^- p$ well

both with and without a bare baryon.

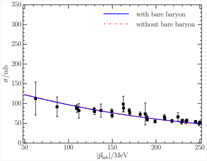

$K^- p \to K^- p$

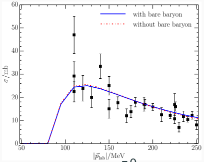

$K^- p \to \bar{K}^0 n$

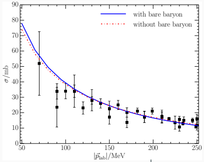

$K^- p \to \pi^- \Sigma^+$

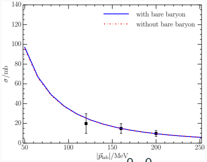

$K^- p \to \pi^0 \Sigma^0$

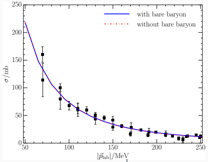

$K^- p \to \pi^+ \Sigma^-$

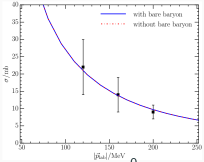

$K^- p \to \pi^0 \Lambda$

Two-pole structure of $\Lambda(1405)$

$1430 - i22$ MeV, $\quad 1338 - i89$ MeV

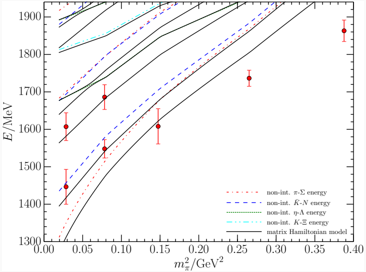

without a bare baryon

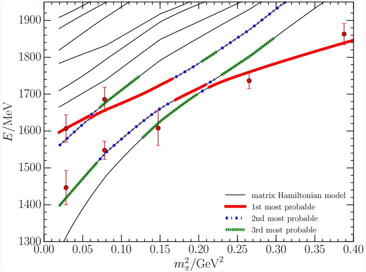

with a bare baryon

Spectra with $S = -1, I(J^P) = 0(\frac{1}{2}^-)$ in the finite volume.

- The bare baryon is important for interpreting the lattice QCD data at large pion masses.
- $\Lambda(1405)$ is mainly a $\bar{K}N$ molecular state

  containing very little of bare baryon at physical pion mass.

Z. W. Liu, J. M. M. Hall, D. B. Leinweber, A. W. Thomas and J. J. Wu, Phys. Rev. D **95** 014506

Kaonic Hydrogen

energy shift and width of 1s level were measured at SIDDHARTA-2

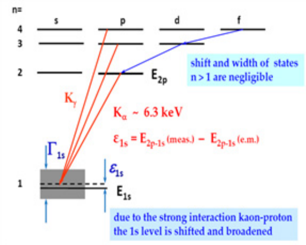

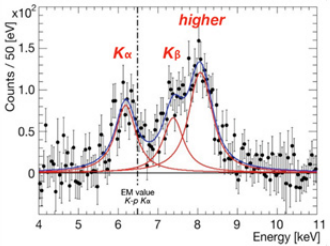

$$
\begin{aligned}
\epsilon_{1s}^{p} &= 283 \pm 36(\text{stat}) \pm 6(\text{sys})\ \text{eV}, \\
\Gamma_{1s}^{p} &= 541 \pm 89(\text{stat}) \pm 22(\text{sys})\ \text{eV}\,,
\end{aligned}
$$

Kaonic Hydrogen

energy shift and width of 1s level were measured at SIDDHARTA-2

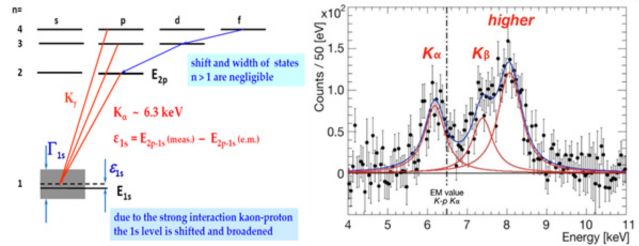

$$\epsilon^p_{1s} = 283 \pm 36(\mathrm{stat}) \pm 6(\mathrm{sys})\ \mathrm{eV},$$
$$\Gamma^p_{1s} = 541 \pm 89(\mathrm{stat}) \pm 22(\mathrm{sys})\ \mathrm{eV},$$

- they are related to the scattering length of $K^- p$

$$\epsilon^p_{1s} - \frac{i}{2}\Gamma^p_{1s} = \frac{-2\alpha_e^3 \mu^2_{K^-p}\, a_{K^-p}}{1 + 2\alpha_e \mu_{K^-p} (\ln \alpha_e - 1)\, a_{K^-p}},$$

"double-improved" Deser formula

Kaonic Hydrogen

energy shift and width of 1s level were measured at SIDDHARTA-2

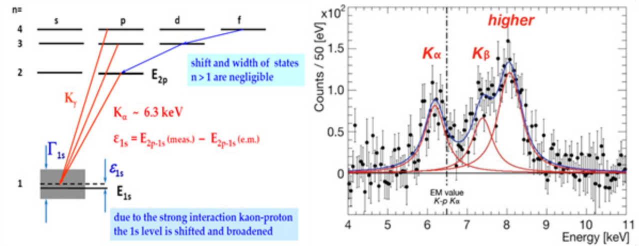

$$
\begin{aligned}
\epsilon_{1s}^{p} &= 283 \pm 36(\mathrm{stat}) \pm 6(\mathrm{sys})\ \mathrm{eV}, \\
\Gamma_{1s}^{p} &= 541 \pm 89(\mathrm{stat}) \pm 22(\mathrm{sys})\ \mathrm{eV},
\end{aligned}
$$

- they are related to the scattering length of $K^- p$

$$
\epsilon_{1s}^{p} - \frac{i}{2}\Gamma_{1s}^{p} = \frac{-2\alpha_e^3\,\mu_{K^-p}^2\,a_{K^-p}}{1 + 2\alpha_e\,\mu_{K^-p}\,(\ln\alpha_e - 1)\,a_{K^-p}},
$$

"double-improved" Deser formula

- With $\bar{K}N$ interactions NOT fine tuned,

HEFT provides

$$
\epsilon_{1s}^{p} = 307\ \mathrm{eV}, \qquad \Gamma_{1s}^{p} = 533\ \mathrm{eV}.
$$

Kaonic Deuteron without Recoil Effect

$\bar{K}NN$ scattering amplitude can be solved by the Faddeev equation

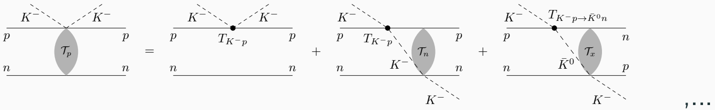

With the static approximation,

$$a_{K^-d} = \frac{m_d}{m_K + m_d} \int d^3\vec{r}\,|\psi_d(\vec{r})|^2\ \hat{A}_{K^-d}(r)\,,$$

where

$$\hat{A}_{K^-d}(r) = \frac{\tilde{a}_{K^-p} + \tilde{a}_{K^-n} + (2\tilde{a}_{K^-p}\tilde{a}_{K^-n} - b_x^2)/r - 2b_x^2\tilde{a}_{K^-n}/r^2}{1 - \tilde{a}_{K^-p}\tilde{a}_{K^-n}/r^2 + b_x^2\tilde{a}_{K^-n}/r^3}\,.$$

Our results without recoil effect are similar to others

$$\epsilon^d_{1S}|_{\text{StaticApprox}} = 855\ \text{eV}, \quad \Gamma^d_{1S}|_{\text{StaticApprox}} = 1127\ \text{eV}\,.$$

Recoil Effect

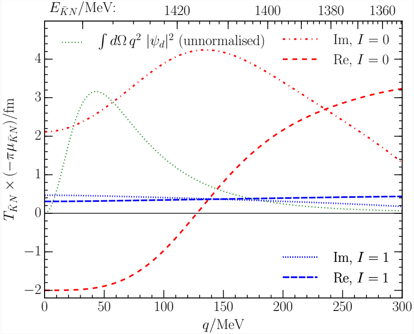

- The recoil effect is mainly from the single scattering process

$$\langle\, T^d_{\bar{K}N} \,\rangle \equiv \int d^3\vec{q}\, |\psi_d(\vec{q})|^2 \;\, T_{\bar{K}N}(\vec{q}).$$

- If no $\Lambda(1405)$ exists,

  this kind of recoil effect can be totally neglected.

Recoil Effect

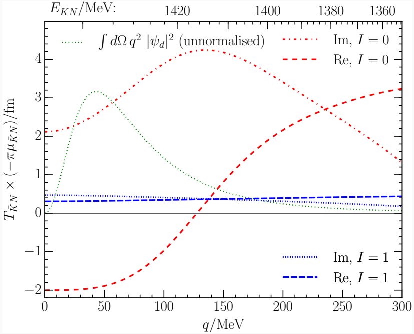

Z. W. Liu, J. J. Wu, D. B. Leinweber and A. W. Thomas, Phys. Lett. B **808** (2020), 135652

- The recoil effect is mainly from the single scattering process

$$\langle T^d_{\bar{K}N} \rangle \equiv \int d^3\vec{q}\, |\psi_d(\vec{q})|^2\; T_{\bar{K}N}(\vec{q}).$$

- If no $\Lambda(1405)$ exists,

  this kind of recoil effect can be totally neglected.

Comparison

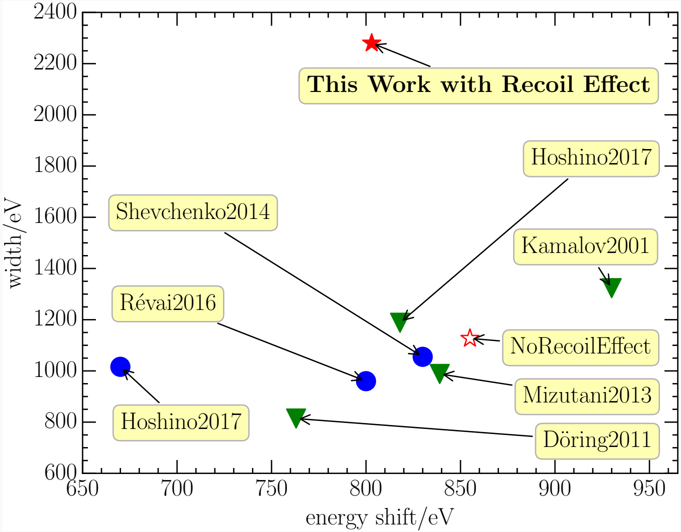

This Work with Recoil Effect
Hoshino2017
Shevchenko2014
Kamalov2001
Révai2016
NoRecoilEffect
Mizutani2013
Hoshino2017
Döring2011
width/eV
energy shift/eV
2400
2200
2000
1800
1600
1400
1200
1000
800
600
650
700
750
800
850
900
950

Kaonic Deuteron scattering length with Recoil Effect

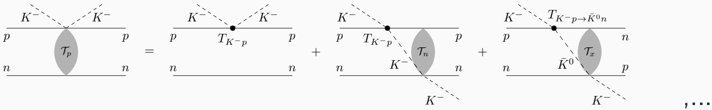

a_{K^-d}	Single Scattering	Single+Multiple Scatterings
Re	-0.06	-0.59
Im	2.55	2.70

The imaginary part of a_{K^-d} is dominant by the simgle scattering diagram.

Summary

Summary

In this report, I have briefly discussed

- the low-lying baryons with Hamiltonian EFT
  - $N^*(1535)$ contains a 3-quark core;
  - $N^*(1440)$ should contain little of 3-quark consistent;
  - $\Lambda(1405)$ is mainly a $\bar{K}N$ molecular state at physical quark mass, while a 3-quark core dominates at large quark masses.
- Energy Shift and Decay Width of Kaonic Deuteron with Hamiltonian EFT
  Recoil effect makes kaonic deuteron much short lived because of the close $\Lambda(1405)$.

Thanks for your attentions!

Backup

Backup

ALICE Collaboration @ LHC have verified our $K^- p$ scattering length

Physics Letters B 822 (2021) 136708

Contents lists available at ScienceDirect

Physics Letters B

www

2366–2382.
[77] Z.-W. Liu, J.-J. Wu, D.B. Leinweber, A.W. Thomas, Kaonic hydrogen and deuterium in Hamiltonian effective field theory, Phys. Lett. B 808 (2020) 135652, arXiv:2003.09181.

Kaon–proton strong interaction at low relative momentum via femtoscopy in Pb–Pb collisions at the LHC

ALICE Collaboration *

ARTICLE INFO

Article history:
Received 29 July 2021
Received in revised form 29 Septem
2021
Accepted 1 October 2021
Available online 6 October 2021
Editor: M. Pierini

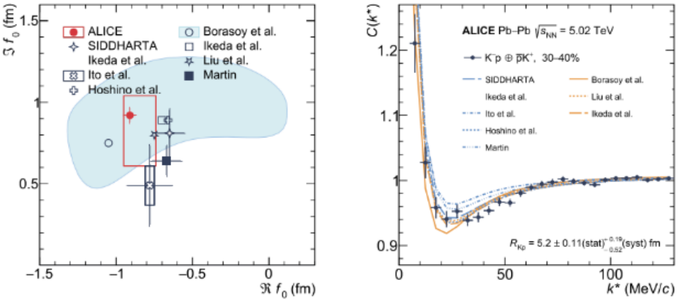

Fig. 3. Left: scattering parameters obtained from the Lednický–Lyuboshitz fit compared with available world data and theoretical calculations. Statistical uncertainties are represented as bars and systematic uncertainties, if provided, as boxes. Right: experimental femtoscopic correlation function for $K^-p \oplus K^+\bar{p}$ pairs in the 30–40% centrality interval, together with various Lednický–Lyuboshitz calculations obtained using the scattering length parameters from Refs. [17,18,75–79] and the source radius from this analysis. The statistical and systematic uncertainties of the measured data points are added in quadrature and shown as vertical bars.